Korean J. Chem. Eng., **23**(4), 678-682 (2006)

Fabrication of high aspect ratio nanostructures using capillary force lithography

Kahp Yang Suh†, Hoon Eui Jeong, Jee Won Park, Sung Hoon Lee and Jae Kwan Kim

School of Mechanical and Aerospace Engineering, Seoul National University, Seoul 151-742, Korea
(*Received 29 November 2005 • accepted 3 February 2006*)

Abstract−A new ultraviolet (UV) curable mold consisting of functionalized polyurethane with acrylate group (MINS101m, Minuta Tech.) has recently been introduced as an alternative to replace polydimethylsiloxane (PDMS) mold for sub-100-nm lithography. Here, we demonstrate that this mold allows for fabrication of various high aspect ratio nanostructures with an aspect ratio as high as 4.4 for 80 nm nanopillars. For the patterning method, we used capillary force lithography (CFL) involving direct placement of a polyurethane acrylate mold onto a spin-coated polymer film followed by raising the temperature above the glass transition temperature of the polymer (T_g). For the patterning materials, thermoplastic resins such as polystyrene (PS) and poly(methyl methacrylate) (PMMA) and a zinc oxide (ZnO) precursor were used. For the polymer, micro/nanoscale hierarchical structures were fabricated by using sequential application of the same method, which is potentially useful for mimicking functional surfaces such as lotus leaf.

Key words: Capillary Force Lithography, Nanostructures, Aspect Ratio, Laplace Pressure

INTRODUCTION

The fabrication of well-defined nanostructures is of great interest due to its potential applications in photonic crystals [Poborchii et al., 1999; Wanke et al., 1997; Yang and Ozin, 2000], data storage [Cheng et al., 2001; Hehn et al., 1996; Krauss and Chou, 1997], and nanometer-scale biological sensors [Haes and Van Duyne, 2002; Lee et al., 2002]. Since the 1990s, unconventional methods such as nanoimprint lithography [Chou et al., 1996] and soft lithography [Lee et al., 2003; Xia and Whitesides, 1998] that enable micro/nano scale patterning on large areas with low cost have been developed as alternatives to conventional photolithography and electron-beam lithography. In such parallel processes, various patterns are simultaneously formed by the physical contact of a hard or a soft mold with the targeted substrate.

Recently, we developed capillary force lithography (CFL) for patterning polymers over large areas by simply combining essential features of nanoimprint and soft lithographies [Khang and Lee, 2004; Kim et al., 2001; Suh et al., 2001; Suh and Lee, 2002]. This technique involves the direct placement of a patterned elastomeric mold such as polydimethylsiloxane (PDMS) onto a spin-coated polymer film on a substrate followed by formation of a negative replica of the mold by raising the temperature above the polymer's glass transition temperature [Suh et al., 2001]. A potential concern in this technique is that a high aspect-ratio sub-100-nm PDMS mold is nearly impossible to obtain due to the low elastic modulus of PDMS (~1.8 MPa) that causes deformation, buckling, and collapse of shallow relief features [Bietsch and Michel, 2000; Delamarche et al., 1997]. To overcome these mechanical shortcomings of PDMS, a number of alternative molds have been introduced such as a composite PDMS [Schmid and Michel, 2000], a bilayer PDMS [Odom et al., 2002], a photocurable PDMS [Choi and Rogers, 2003], a polyolefin mold [Csucs et al., 2003], a PDMS with polymer-reinforced sidewalls [Suh et al., 2003], a Teflon mold [Khang et al., 2004; Khang and Lee, 2004], and a photocurable polyurethane acrylate mold [Choi et al., 2004; Kim et al., 2003]. Of these, the polyurethane acrylate (PUA) mold turned out to be stiff enough for replicating dense sub-100-nm features. In addition, the mold allows for flexibility that is capable of large area replication and a tunable modulus, enabling from imprinting to microcontact printing.

Here, we report that this PUA mold can be used in CFL with slight modification of the experimental protocol for fabricating high-aspect ratio nanostructures, drastically expanding the flexibility of the method. Due to the ability to fabricate high-aspect ratio structures, multiscale hierarchical structures were created with superior wetting properties, providing a simple way to mimicking many functional surfaces found in nature such as lotus leaf. It is believed that the micro/nanoscale hierarchical structure is considered to be an optimized building block for natural surfaces. Furthermore, a zinc oxide (ZnO) precursor was used for the fabrication to test the applicability of inorganic materials, which turned out to be successful as shown shortly.

EXPERIMENTAL

1. Fabrication of PUA Mold

The PUA mold was composed of a functionalized prepolymer with acrylate groups for crosslinking, a monomeric modulator, a photoinitiator and a radiation-curable releasing agent for surface activity. The liquid mixture was drop-dispensed onto a silicon master that had been prepared by electron beam lithography, and a transparent polyethylene terephthalate (PET) film with 50 mm thickness was gently placed on the liquid mixture followed by UV (λ= 250-400 nm) exposure for a few tens of seconds. After the UV curing, the mold was peeled off from the master [Choi et al., 2004].

2. Capillary Force Lithography (CFL)

For fabricating polymer nanostructures, silicon wafer was cleaned by ultrasonic treatment in trichloroethylene and methanol for 5 min each and dried in nitrogen. For the polymer, we used commercial polystyrene (PS) (M_w=2.3×10^5, T_g=100 °C, Aldrich) and poly(methyl-

†To whom correspondence should be addressed.
E-mail: sky4u@snu.ac.kr

methacrylate) (PMMA) (M_w=1.2×10^5, T_g=105 °C, Aldrich) dissolved in toluene (10 wt%). The PS or PMMA polymer was spin-coated onto the silicon substrate and the PUA mold was placed on the polymer surface under a slight pressure (~10 g/cm^2) for conformal contact with the polymer. For a uniform pressure distribution, a thin PDMS block was placed as a buffer on top of the PUA mold prior to the application of pressure. Then the sample was annealed at 150 °C, well above the glass transition temperature for 30 min on a hot stage.

For fabricating polymer multiscale hierarchical structures, a patterned PDMS mold was placed onto the spin-coated polymer surface on the silicon substrate. Then the sample was annealed at 150 °C for 1 hr on a hot stage After a microstructure was fabricated, the PUA mold was placed on the as-prepared microstructure under a slight pressure (~10 g/cm^2) for conformal contact with the polymer. Then the polymer was annealed again at 120 °C for 5 min on a hot stage to fabricate nanostructures.

A ZnO precursor was used as an inorganic patterning material. ZnO precursor solution was prepared according to the well-known methods [Choy et al., 2003]. Then the silicon substrate was spin-coated by the prepared precursor solution. Patterned PUA molds were then placed under a slight pressure (~10 g/cm^2) and the sample was annealed at 250 °C for 5 hours.

3. Contact Angle Measurements

The static contact angle (CA) of water was measured by a contact angle analyzer (Phoenix 150, Surface Electro Optics Co., Korea) and the presented values were averaged over at least six points.

4. Scanning Electron Microscopy (SEM)

Images were taken with high-resolution SEM (XL30FEG, Philips Electron Co., Netherlands) at an acceleration voltage of 3 eV and a working distance of 7 mm. Samples were coated with a 30 nm Au layer prior to analysis to prevent charging.

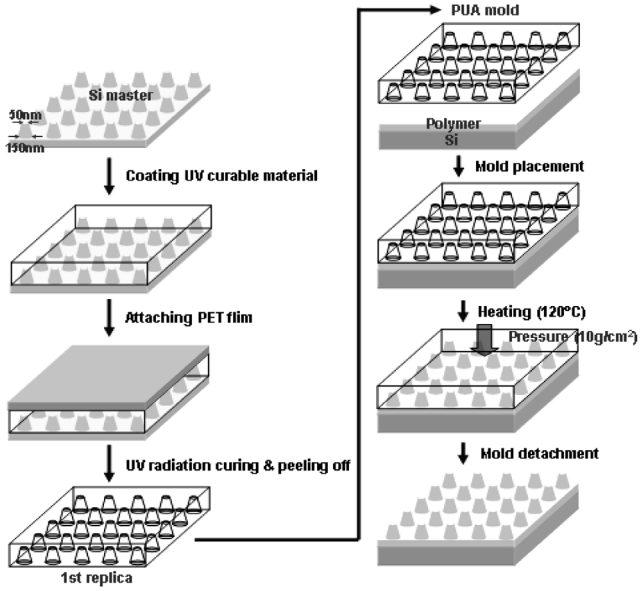

Fig. 1. A schematic of the molding procedure. The PUA mold used in the experiment is a negative thin sheet type mold (features sticking in).

RESULTS AND DISCUSSION

Fig. 1 shows a schematic diagram of the patterning procedure.

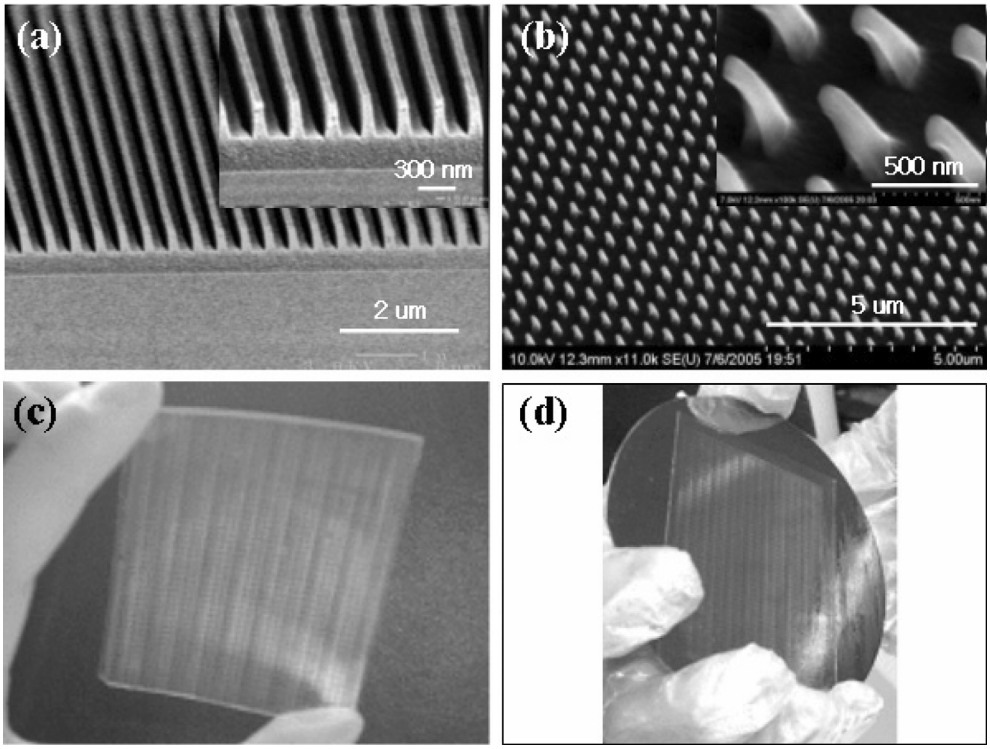

Fig. 2. (a-b) SEM images of high aspect ratio (AR) nanostructures: (a) Nanolines (AR=4.4) with the width of ~80 nm and the spacing of ~270 nm. (b) Nanopillars (AR=3.4) with 150-200 nm width at base, 70-100 nm width at top and ~420 nm height. (c-d) Optical images of the sheet type mold (c) and the same mold supported on silicon substrate (d).

A negative PUA mold was precisely replicated by exposing the uncured PUA on the complementary, nanopatterned Si master to UV [Choi et al., 2004]. The PUA mold obtained was not only flexible (~50 μm thickness) but also sufficiently hard (tensile modulus of ~40 MPa). The film type PUA mold aids to make a conformal contact with low pressure (~10 g/cm^2) compared to nanoimprint lithography [Chou et al., 1996] and to expel the trapped air more easily at the time of contact, enabling a large-area fabrication [Khang et al., 2004].

Fig. 2 shows typical SEM images of the patterned PS nanolines (a) and PMMA nanopillars (b). The inset images show an enlarged view, indicating the presence of the well defined, densely packed nanolines or nanopillars. The aspect ratio of the nanolines is 4.4 with a width of ~80 nm and spacing of ~270 nm. The nanopillar is truncated cone shape, with 150-200 nm width at base, 70-100 nm width at top and ~420 nm height. An example of the sheet type mold and the same mold supported on silicon substrate are shown in Figs. 1(c) and (d), respectively.

To gain an understanding of the capillary rise, we calculated a Laplace pressure for the polymer within the void space of 150 nm in diameter, which gives

$$\Delta P_L = \frac{2\gamma}{r}\cos\theta \approx \frac{2\times 43\ \mathrm{mJ/m^2}}{75\ \mathrm{nm}}\cos 33^\circ = 9.62\ \mathrm{atm} \quad (1)$$

where ΔP_L is the Laplace pressure, γ is the surface tension of PMMA [Brandup and Immergut 1989], r is the radius of the void, and θ is the contact angle at the air/PUA/PMMA interface, which was independently calculated as described in the literature [Seo et al., 2005; Wu, 1982]. This is a rough estimation of the pressure since the effects of a slanted wall and non-uniformly curved meniscus were not taken into consideration. The actual Laplace pressure would be somewhat smaller. Using the calculated Laplace pressure, the maximum possible height of the capillary rise can be estimated. The initial air pressure within the void space is 1.4 atm at 150 °C assuming ideal gas behavior, which would proportionally increase with increasing capillary rise. For example, the hydrodynamic pressure increases to 2.8 atm if the polymer rises up to the half height of the mold, assuming no air permeation. Thus, the maximum height h_{max}, which is a function of the original height of the mold, results by equating the Laplace and the increased hydrodynamic pressures. For the conditions used in the experiment, we obtained $h_{max} \approx (6/7)\cdot h$ (initial height) ≈ 430 nm, in excellent agreement with our observations.

With the aid of the PUA mold, we were also able to fabricate micro/nanoscale hierarchical structures using CFL. It is worthwhile noting that micro/nanoscale hierarchical structure is not easily accessible or not economically viable with other methods. For example, photolithography requires a two-step process with application of a microscale mask followed by a nanoscale mask, which is not cost-effective and would suffer from swelling or deformation of the pre-formed microstructure. Moreover, nanoimprint lithography [Chou et al., 1996] is a simple and yet robust technique for fabricating nanostructures with moderate aspect ratio but is not directly applied to the fabrication of high aspect ratio microstructures. To enable the fabrication, we adopted a two-step capillary force lithography involving a sequential application of molding process where a uniform polymer film is molded by a pre-defined pattern of the mold by means of capillary force above the T_g of the polymer [Suh et al., 2001]. The two steps consist of (i) microfabrication of polymer structures using a low-resolution, micropatterned polydimethylsiloxane (PDMS) mold and (ii) subsequent nanofabrication using a high-resolution nanopatterned polyurethane acrylate (PUA) mold on top of

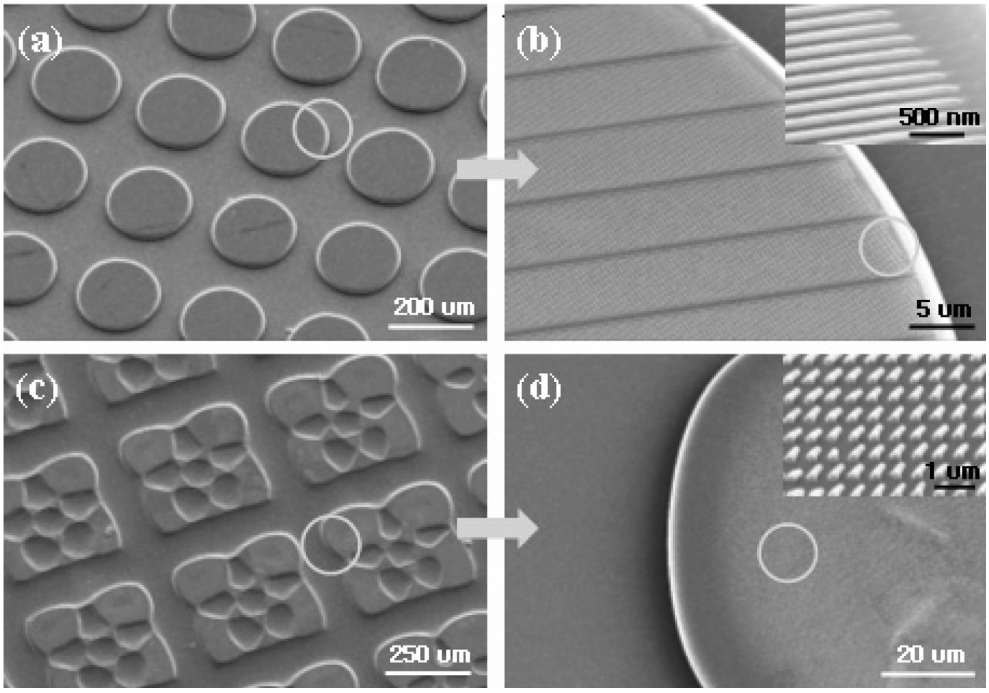

Fig. 3. SEM images of multiscale hierarchical structures: (a-b) Nanolines with ~70 nm in width and ~150 nm in height on top of 100 μm cylinder posts. (c-d) Nanopillars with ~100 nm in diameter and ~400 nm in height on the pre-formed microstructures.

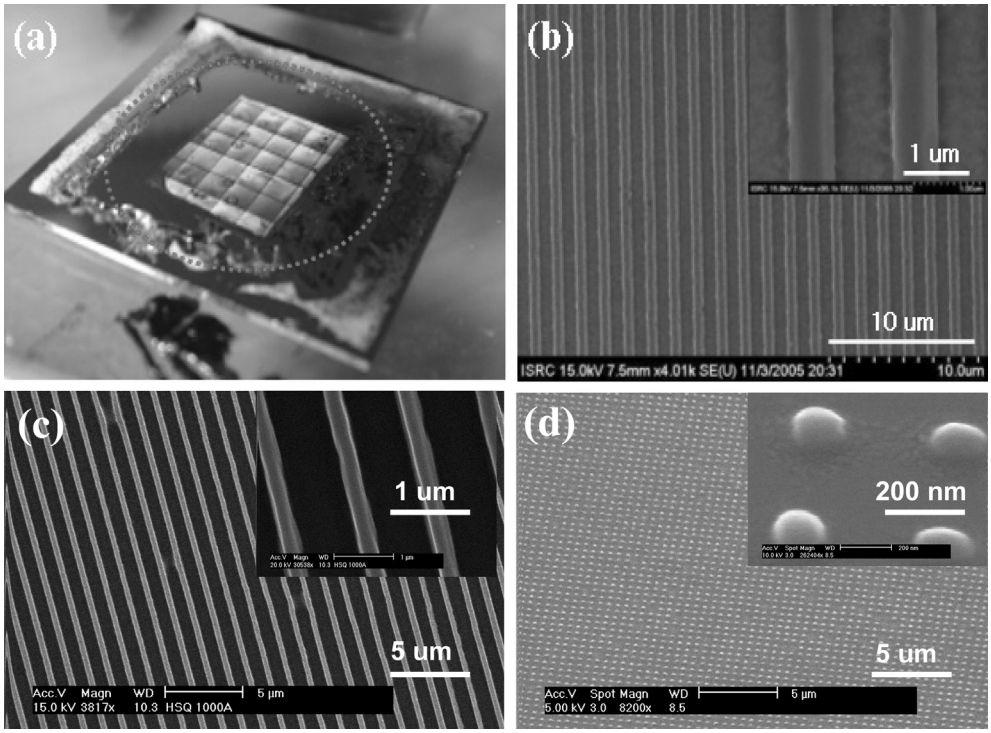

Fig. 4. (a) An optical image of large-area fabrication (1.5×1.5 cm^2). (b)-(d) SEM image of (b-c) ZnO nanolines [~700 nm in width and ~1.1 μm in height for (b), ~300 nm in width and ~1.1 μm in height for (c)] and (d) nanospheres (~150 nm in diameter and ~270 nm in height).

the pre-formed polymer microstructures. Fig. 3 shows SEM images of two kinds of combined structures. The patterned nanolines on the micro circles shown in Fig. 3(a) and (b) have ~70 nm in width and ~150 nm in height. Figs. 3(c) and (d) show patterned nanopillars with ~100 nm in diameter and ~400 nm in height on the pre-formed microstructures. It is noted that temperature and heating time were two crucial factors for the successful two-step capillary molding process. In order to minimize the deformation of the pre-defined microstructure, temperature was typically maintained at 120 °C (just above T_g of ~100 °C for PS and ~105 °C for PMMA) for a short period of time (~5 min). Otherwise, a substantial collapse or deformation of the pre-formed microstructure was observed (not shown).

The multiscale hierarchical structures presented here are potentially useful for studying nature's functional surfaces. A typical example is the surface of a lotus leaf where the surface roughness caused by the micrometer-scale papillae and the epicuticular wax exhibits unusual super-hydrophobic wetting properties with self-cleaning effect [Ball, 1999; Neinhuis and Barthlott, 1997]. A recent finding revealed that micro/nanoscale hierarchical structures are found on the surface of a lotus leaf, which further increases wetting angle and reduces sliding angle or the difference between advancing and receding contact angles [Feng et al., 2002]. Motivated by this fact, we measured contact angles on different surfaces to examine the effects of multiscale structures. The initial PS surface rendered a contact angle of 86°. On top of PS microstructures in the absence of nanostructures, the apparent contact angle was increased to 104-115°. Finally, on top of micro/nanoscale combined structures, the measured values were 117-126°, suggesting that the multiscale structures are useful for fabricating more hydrophobic surfaces. Future work needs to address this issue in detail.

We further investigated the possibility of patterning inorganic nanostructures by using the same process. Examples of patterned ZnO nanostructures on silicon substrate are shown in Fig. 4. As shown in Fig. 4(a), we were able to fabricate well-defined ZnO nanostructures on a large area (1.5×1.5 cm^2). Figs. 4(b)-(d) show the SEM images of (b-c) ZnO nanolines [~700 nm in width and ~1.1 μm in height for (b), ~300 nm in width and ~1.1 μm in height for (c)] and (d) nanospheres (~150 nm in diameter and ~270 nm in height). Although further work is necessary to establish the pattering of inorganic materials, these results indicate the applicability of robust inorganic structures for future etching resists or device materials.

SUMMARY

We have presented the fabrication of high-aspect nanostructures with the aid of high-resolution UV curable PUA mold. It was shown that CFL enables large-area nanopatterning of organic (PS and PMMA) and inorganic (ZnO) materials under a slight pressure for making conformal contact. The PUA mold was hard yet flexible, allowing for sub-100-nm patterning on a large area. It is hoped that this simple method would provide a versatile, economically viable route for fabricating various micro or nanostructures for potential applications to micro/nanoscale devices.

ACKNOWLEDGEMENT

This work was supported by the Ministry of Science and Technology through the Nanoscopia Center of Excellence at Seoul Na-

tional University and supported in part by the Micro Thermal System Research Center of Seoul National University.

REFERENCES

Ball, P., "Engineering - Shark skin and other solutions," *Nature*, **400**, 507 (1999).

Bietsch, A. and Michel, B., "Conformal contact and pattern stability of stamps used for soft lithography," *J. Appl. Phys.*, **88**, 4310 (2000).

Brandup, J. and Immergut, E. H., *Polymer Handbook*, Wiley, New York (1989).

Cheng, J. Y., Ross, C. A., Chan, V. Z. H., Thomas, E. L., Lammertink, R. G. H. and Vancso, G. J., "Formation of a cobalt magnetic dot array via block copolymer lithography," *Adv. Mater.*, **13**, 1174 (2001).

Choi, K. M. and Rogers, J. A., "A photocurable poly(dimethylsiloxane) chemistry designed for soft lithographic molding and printing in the nanometer regime," *J. Am. Chem. Soc.*, **125**, 4060 (2003).

Choi, S. J., Yoo, P. J., Baek, S. J., Kim, T. W. and Lee, H. H., "An ultraviolet curable mold for sub-100 nm lithography," *J. Am. Chem. Soc.*, **126**, 7744 (2004).

Chou, S. Y., Krauss, P. R. and Renstrom, P. J., "Imprint lithography with 25-nanometer resolution," *Science*, **272**, 85 (1996).

Choy, J. H., Jang, E. S., Won, J. H., Chung, J. H., Jang, D. J. and Kim, Y. W., "Soft solution route to directionally grown ZnO nanorod arrays on Si wafer; room-temperature ultraviolet laser," *Adv. Mater.*, **15**, 1911 (2003).

Csucs, G., Kunzler, T., Feldman, K., Robin, F. and Spencer, N. D., "Microcontact printing of macromolecules with submicrometer resolution by means of polyolefin stamps," *Langmuir*, **19**, 6104 (2003).

Delamarche, E., Schmid, H., Michel, B. and Biebuyck, H., "Stability of molded polydimethylsiloxane microstructures," *Adv. Mater.*, **9**, 741 (1997).

Feng, L., Li, S. H., Li, Y. S., Li, H. J., Zhang, L. J., Zhai, J., Song, Y. L., Liu, B. Q., Jiang, L. and Zhu, D. B., "Super-hydrophobic surfaces: From natural to artificial," *Adv. Mater.*, **14**, 1857 (2002).

Haes, A. J. and Van Duyne, R. P., "A nanoscale optical biosensor: Sensitivity and selectivity of an approach based on the localized surface plasmon resonance spectroscopy of triangular silver nanoparticles," *J. Am. Chem. Soc.*, **124**, 10596 (2002).

Hehn, M., Ounadjela, K., Bucher, J. P., Rousseaux, F., Decanini, D., Bartenlian, B. and Chappert, C., "Nanoscale magnetic domains in mesoscopic magnets," *Science*, **272**, 1782 (1996).

Khang, D. Y., Kang, H., Kim, T. and Lee, H. H., "Low-pressure nanoimprint lithography," *Nano. Lett.*, **4**, 633 (2004).

Khang, D. Y. and Lee, H. H., "Pressure-assisted capillary force lithography," *Adv. Mater.*, **16**, 176 (2004).

Kim, Y. S., Lee, H. H. and Hammond, P. T., "High density nanostructure transfer in soft molding using polyurethane acrylate molds and polyelectrolyte multilayers," *Nanotechnology*, **14**, 1140 (2003).

Kim, Y. S., Suh, K. Y. and Lee, H. H., "Fabrication of three-dimensional microstructures by soft molding," *Appl. Phys. Lett.*, **79**, 2285 (2001).

Krauss, P. R. and Chou, S. Y., "Nano-compact disks with 400 Gbit/in(2) storage density fabricated using nanoimprint lithography and read with proximal probe," *Appl. Phys. Lett.*, **71**, 3174 (1997).

Lee, K. B., Kim, D. J., Yoon, K. R., Kim, Y. and Choi, I. S., "Patterning Si by using surface functionalization and microcontact printing with a polymeric ink," *Korean J. Chem. Eng.*, **20**, 956 (2003).

Lee, K. B., Park, S. ., Mirkin, C. A., Smith, J. C. and Mrksich, M., "Protein nanoarrays generated by dip-pen nanolithography," *Science*, **295**, 1702 (2002).

Neinhuis, C. and Barthlott, W., "Characterization and distribution of water-repellent, self-cleaning plant surfaces," *Ann. Bot.*, **79**, 667 (1997).

Odom, T. W., Love, J. C., Wolfe, D. B., Paul, K. E. and Whitesides, G. M., "Improved pattern transfer in soft lithography using composite stamps," *Langmuir*, **18**, 5314 (2002).

Poborchii, V. V., Tada, T. and Kanayama, T., "A visible-near infrared range photonic crystal made up of Si nanopillars," *Appl. Phys. Lett.*, **75**, 3276 (1999).

Schmid, H. and Michel, B., "Siloxane polymers for high-resolution, high-accuracy soft lithography," *Macromolecules*, **33**, 3042 (2000).

Seo, S. M., Park, J. Y. and Lee, H. H., "Micropatterning of metal substrate by adhesive force lithography," *Appl. Phys. Lett.*, **86**, (2005). As described in this paper, we used the relation $\gamma_l(1+\cos\theta)=2(\gamma_s^d\gamma_l^d)^{1/2}+2(\gamma_s^p\gamma_l^p)^{1/2}$ to estimate the contact angle of PMMA on PUA mold (θ), where the superscripts d and p are for the dispersion and polar components of the surface tension γ. Calculated dispersion and polar components surface tensions of PUA mold and PMMA are as follows: γ_{PUA}^d=21.6, γ_{PUA}^p=33.3 (PUA=solid), γ_{PMMA}^d=39.89, γ_{PMMA}^p=3.17 mJ/m^2 (PMMA=liquid). From these values, θ=33.3° was obtained.

Suh, K. Y., Kim, Y. S. and Lee, H. H., "Capillary force lithography," *Adv. Mater.*, **13**, 1386 (2001).

Suh, K. Y., Langer, R. and Lahann, J., "Fabrication of elastomeric stamps with polymer-reinforced sidewalls via chemically selective vapor deposition polymerization of poly(p-xylylene)," *Appl. Phys. Lett.*, **83**, 4250 (2003).

Suh, K. Y. and Lee, H. H., "Capillary force lithography: Large-area patterning, self-organization, and anisotropic dewetting," *Adv. Funct. Mater.*, **12**, 405 (2002).

Wanke, M. C., Lehmann, O., Muller, K., Wen, Q. Z. and Stuke, M., "Laser rapid prototyping of photonic band-gap microstructures," *Science*, **275**, 1284 (1997).

Wu, S., *Polymer Interface and Adhesion*, Dekker, New York (1982).

Xia, Y. N. and Whitesides, G. M., "Soft lithography," *Annu. Rev. Mater. Sci.*, **28**, 153 (1998).

Yang, S. M. and Ozin, G. A., "Opal chips: vectorial growth of colloidal crystal patterns inside silicon wafers," *Chem. Comm.*, **24**, 2507 (2000).